New Design for Efficient Diesel Particulate Trap Regeneration

Haishan Zheng and Jason M. Keith
Dept. of Chemical Engineering, Michigan Technological University, Houghton, MI 49931

Using numerical simulations shows that particulate trap regeneration does not occur below a certain critical inlet temperature, 679 K, for a typical diesel exhaust mass flow rate of 0.0523 kg/s. A new bypass design for particulate trap regeneration has been studied, where the exhaust flow is divided into several channels, which results in a smaller flow rate in each particulate filter. This reduces the critical inlet temperature by 20 K to 40 K, depending on the number of channels, and allows for improved regeneration efficiency with low electric energy consumption. In addition, a zero-order analytical estimate for the ignition time is also developed, given by $u_{ig} = 2.50/\xi + \ln|r_i| - 0.344$, *where* u_{ig} *is a dimensionless ignition time,* r_i *is a reduced temperature, and* ξ *depends upon feed temperature, flow rate, oxygen concentration, and initial deposit thickness. An optimal design using three bypass channels is obtained by theory and simulation.* © 2004 American Institute of Chemical Engineers *AIChE J,* 50: 184–191, 2004
Keywords: particulate trap, thermal regeneration, numerical modeling, diesel engine, bypass design

Introduction

Unlike gasoline engines, diesel engines emit large amounts of particulate matter, a mixture of carbon nuclei carrying absorbed sulphates, metal oxides, and hydrocarbons. It has been widely recognized that particles smaller than 2.5 μm play a key role in contributing to heart and lung diseases (Muscat and Wynder, 1995). For this reason, governments are tightening particulate emission limits. Although advanced diesel engine design has resulted in much "cleaner" engines, a particulate filter is still needed to meet the strict regulations of the future.

The most efficient filter is the wall-flow monolith particulate filter in which each channel is opened at one end and closed at the opposite end, forcing exhaust flow through the porous channel wall (Howitt and Montierth, 1981). To avoid unacceptable levels of backpressure, it is necessary to clean the filter periodically by oxidizing or "regenerating" the collected particulates, which without catalytic aids requires high exhaust temperatures. Thus, various regeneration techniques have been employed to start the combustion of the collected soot particles.

One popular regeneration technique is thermal regeneration by use of an upstream electric heater. Arai and Miyashita (1990) and Igarashi et al. (1991) described the development of a filter system using an electric heater, which draws electricity from the vehicle battery, heating the exhaust flow to initiate regeneration. However, due to the high exhaust flow rate, this system still faces difficulty in raising the exhaust temperature above the temperature necessary for regeneration.

One way to solve this problem is to reduce the exhaust flow through the particulate filter. This is accomplished in this article by the use of a bypass configuration, where the exhaust flow is divided into more than one channel, which results in a smaller flow rate in each channel. A first-stage study of the bypass filtration system with the aid of a popular and simple numerical model (Bissett and Shadman, 1985) and an analytical estimate for the ignition time are reported.

Model Formulation

In this study, heat is added to the exhaust gas by an auxiliary electric heater. In agreement with the current implementation,

Correspondence concerning this article should be addressed to J. M. Keith at jmkeith@mtu.edu.

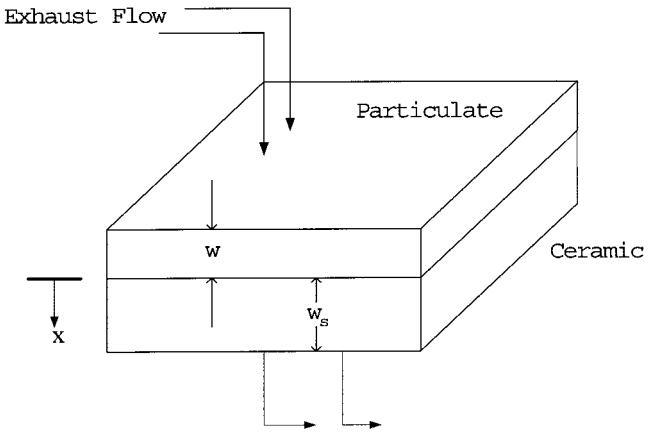

Figure 1. Model geometry for a section of the filtration area.

the electric heater is physically separated from the particulate filter. In this study we only consider the configuration of an upstream electric heater followed by a downstream monolithic filter. There is a small air gap between these two segments.

This configuration results in two zones: the heated zone, in which there is no filtration, and the unheated zone, in which filtration of particulates occurs, followed by a reaction. We can formulate a two-zone model: a filter model and an electric-heater model, in which all the physical and chemical properties of each zone can be specified separately.

Filter Model Formulation

A fairly large number of computer models for thermal regeneration processes have been reported in the past 20 years. The classic work of Bissett and Shadman (1985) with a transient, position-independent model is the most common model referenced in the literature. Broadly speaking, this simple model predicts the temperature in both the gas and solid phases as a function of time. The model developed in their article considers that the gas flows through two layers: the particle deposit, which shrinks with time during regeneration, and the porous channel wall, which remains unchanged (Figure 1).

The model assumes a uniform flow distribution at the monolith face and adiabatic operation of the monolithic filter. Under these assumptions, all channels behave the same, thus allowing for consideration of only one channel. This model employs a single spatial variable, x. All variations of temperature and concentration in the directions perpendicular to the x-direction are neglected. The assumption of constant, position-independent gas flow through the porous monolith wall is reasonable if the combined flow resistance of the porous ceramic walls and the particle deposit is much greater than the flow resistance of the open monolith channels. Also, since the conductive heat transfer between the channel gas and the monolith walls is negligible compared to convective transport in the channels for sufficiently high exhaust flow rates, the deposit layer is exposed to a uniform temperature throughout the regeneration process. However, in an effort to determine robust analytical ignition criteria, the assumption of no axial temperature gradients is being tested with a more detailed model, the results of which will be reported in a later study.

A uniformly shrinking thickness model, assuming a constant density soot layer, is the most commonly used in the literature (Bissett and Shadman, 1985; Koltsakis and Stamatelos, 1996; Huynh et al., 2003), and it is used here. This model provides good agreement between simulations and experimental data. Other assumptions in this model include neglecting the addition of particles to the deposit during regeneration, and neglecting temperature gradients between the gas and solid phase within the deposit or ceramic substrate.

With the objective of assessing the feasibility and utility of the proposed bypass filtration concept, the simple model of Bissett and Shadman is employed in this article. Their model will be used to describe our new design, which outperforms the standard filter.

Mass exchange between the gas phase and reactant is negligible compared to the convection mass flux. The conservation of mass in the gas phase can thus be represented by the following equation

$$\rho v = F(t)/S \tag{1}$$

where ρ is the gas density, S is the filtration area, v is the gas velocity, and $F(t)$ is the mass flow rate. Assuming that the main reaction through the soot layer is first order with respect to oxygen concentration, and that diffusion is negligible compared to convection, the oxygen balance equation in terms of the oxygen mass fraction y can be written as

$$\frac{\partial}{\partial x}(\rho v y) = -s_j k_j \rho y \qquad j = 1 \text{ (particulate)}, 2 \text{ (ceramic)} \tag{2}$$

where S_j is the specific area of the region j, k_j is the rate coefficient for the reaction in region j, and y is the oxygen mole fraction.

Since there is no reaction in the ceramic layer, $k_2 = 0$, the coefficient k_1 is given by (Field et al., 1967)

$$k_1 = kTe^{(-E/RT)} \tag{3}$$

Assuming that the gas temperature is equal to that of the solid phase, except at the inlet face of the deposit layer, and assuming adiabatic operation, the energy balance equation becomes

$$\rho_j C_{pj} \frac{\partial T}{\partial t} = s_j(-\Delta H/M_a)k_j \rho y + \frac{\partial}{\partial x}\left(\lambda_j \frac{\partial T}{\partial x}\right) - \rho v C_{pg} \frac{\partial T}{\partial x} \tag{4}$$

where accumulation of thermal energy is balanced by the reaction, thermal diffusion, and convection.

Finally, the corresponding rate of shrinkage of the deposit layer is proportional to the rate of oxygen reaction

$$\rho_1 \frac{dw}{dt} = (M_c/M_a)[F(t)/S][y|_{x=0} - y|_{x=-w}] \tag{5}$$

where w is the thickness of the deposit layer, M_c is the atomic weight of the deposit, and M_a is the molecular weight of the exhaust gas.

The initial conditions for this system are prescribed as

$$T(x, t = 0) = T_b, \qquad w(t = 0) = w_b \tag{6}$$

with boundary conditions at $x = -w$

$$y = y_i(t) \tag{7}$$

$$\lambda_1 \frac{\partial T}{\partial x} = \rho v C_{pg}[T - T_i(t)] \tag{8}$$

and at $x = w_s$

$$\frac{\partial T}{\partial x} = 0 \tag{9}$$

where $y_i(t)$ is the mole fraction of oxygen at the inlet, $T_i(t)$ is the inlet temperature, and w_s is the thickness of the monolith channel wall.

Equations 1–5 are rendered dimensionless and solved using a perturbation expansion of T, y, and w. This procedure will be illustrated for the energy conservation equation. Equation 4 is rendered dimensionless to yield

$$\overline{C_{pj}} \frac{\partial \bar{T}}{\partial \bar{t}} = \frac{1}{\delta} \frac{\partial}{\partial \bar{x}} \left(\overline{\lambda_j} \frac{\partial \bar{T}}{\partial \bar{x}} \right) + \overline{\Delta H}\, \overline{k_j}(\bar{T})\, y/\bar{T} - \bar{F} \frac{\partial \bar{T}}{\partial \bar{x}} \tag{10}$$

where $\delta = (C_{pg}F(0)w_b)/S\lambda_1$ is a key dimensionless group.

The $O(\delta)$ term for the energy balance is given as

$$\overline{C_{pj}} \frac{\partial T_0}{\partial \bar{t}} = \frac{\overline{\Delta H}\, \overline{k_j}}{T_0} y_0 + \overline{\lambda_j} \frac{\partial^2 T_1}{\partial \bar{x}^2} \tag{11}$$

with boundary conditions $(\partial T_1/\partial \bar{x}) = \bar{F}(T_0 - \bar{T}_i)$ at $\bar{x} = -w_0$ and $(\partial T_1/\partial \bar{x}) = 0$ at $\bar{x} = \overline{w_s}$, where T_0 is the first term of a perturbation expansion of $\bar{T}$, w_0 is the first term of a perturbation expansion of $\bar{w}$, and y_0 is the first term of a perturbation of y.

The convection term $\bar{F}(\partial T_0/\partial \bar{x})$ in Eq. 11 is ignored since T_0 is found at $O(1)$ to be independent of $\bar{x}$. Upon substitution of $(\bar{k}_j y_0/T_0) = -\bar{F}(\partial y/\partial \bar{x})$ from the $O(1)$ expansion of the dimensionless oxygen balance for the reaction rate, the equation can be integrated from $\bar{x} = -w_0$ to $\overline{w_s}$. After inserting the expression for the oxygen profile, y_0, one obtains

$$\frac{dT_0}{d\bar{t}} = \frac{\bar{F}(\bar{t})}{\overline{C_{p1}}w_0 + \overline{C_{p2}w_s}} \times \left\{ \overline{\Delta H} y_i(\bar{t}) \left[1 - \exp\left(-\frac{\bar{k}(T_0)w_0}{T_0 \bar{F}(\bar{t})} \right) \right] + \bar{T}_i(\bar{t}) - T_0 \right\} \tag{12}$$

Table 1. Filter Parameters

Parameter	Value
S	1.63 m^2
w_s	4.32×10^{-4} m
C_{p2}	1.11×10^3 J/kg · K
ρ_2	1.4×10^3 kg/m^3

Table 2. Standard Initial Conditions, With a Constant Initial Deposit Thickness for all Designs

Initial Conditions	Value
$F(0)$	5.23×10^{-2} kg/s
m	0.02 kg
T_b	606 K
$y_i(0)$	0.052

where $\bar{T}_i$ is the dimensionless inlet temperature.

Similarly, for the deposit thickness one obtains

$$\frac{dw_0}{d\bar{t}} = -\bar{M}\bar{F}(\bar{t})\, y_i(\bar{t}) \left[1 - \exp\left(-\frac{\bar{k}(T_0)w_0}{T_0 \bar{F}(\bar{t})} \right) \right] \tag{13}$$

Equations 12 and 13 are solved subject to the initial conditions $T_0(\bar{t} = 0) = 1$ and $w_0(\bar{t} = 0) = 1$. More details of the derivation may be found in Bissett and Shadman (1985).

Filter Model Dynamic Simulation Results

Table 1 lists the parameters for the standard filter studied by Bissett and Shadman (1985). The initial conditions listed in Table 2 are referred to as the standard initial conditions. We will use these data in numerical simulations for both the standard system and the new bypass system design.

As Figure 2 shows, there are four dynamic stages during the regeneration process: preheating, ignition, transport-controlled combustion, and quenching. It is worth mentioning that the inlet temperature is higher than the deposit temperature in the preheating stage and lower than the deposit temperature in the last three stages. This means that the exhaust flow cools the deposit during most of the regeneration process. This cooling mechanism is the main reason why the standard system has a poor regeneration performance.

By selecting a constant inlet temperature, T_i, in our model simulation, it was found that there exists a critical inlet temperature necessary to initiate ignition of the standard model, leading to complete soot combustion. As Figure 3 shows, the

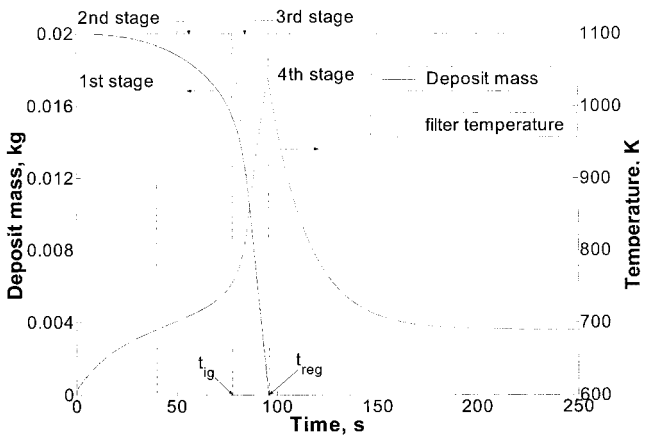

Figure 2. The four stages of the regeneration process.

The ignition time, t_{ig}, is defined by extrapolating the mass vs. time graph from 0.00 kg to 0.02 kg (Lahaye et al., 1996). The regeneration time, t_{reg}, is defined where the temperature reaches a maximum (in this example, t_{ig} = 78 s and t_{reg} = 95.6 s).

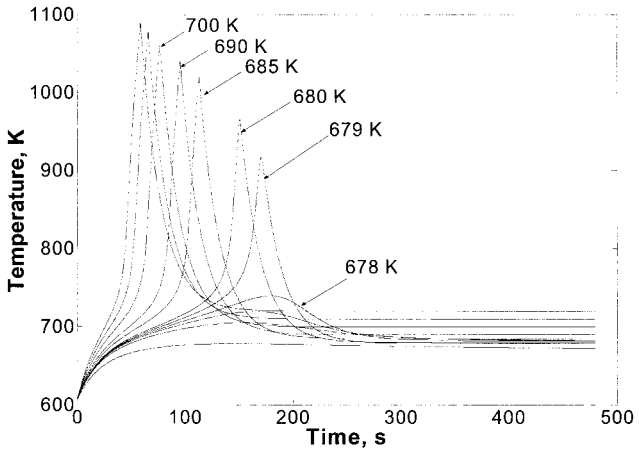

Figure 3. Regeneration dynamics at different feed temperatures.

reaction is ignited and leads to a complete combustion when the inlet temperature is above 679 K for the standard initial conditions. When the inlet temperature is below 679 K, there is no ignition, which results in incomplete regeneration. This is because the deposit temperature exceeds the inlet temperature and the gas cools the deposit during the ignition stage. At the beginning of the ignition stage, the deposit temperature increases because the heat generation by reaction is larger than the heat dissipation by the exhaust gas. With increasing deposit temperatures, the heat dissipation by the exhaust gas increases. For inlet temperatures below 679 K, the heat dissipation by the exhaust gas will exceed the heat generated by reaction, which results in failure to ignite during regeneration. This means that the electric heater must raise the inlet temperature above 679 K to provide complete regeneration in a standard thermal regeneration system.

Electric-heater model formulation and simulation results

As the preceding results indicate, the inlet temperature must be greater than 679 K to initiate regeneration in the standard filter. However, the exhaust-gas temperature is rarely high enough under normal driving conditions. Thus, it is necessary to provide auxiliary energy to the exhaust gas from an electric heater. In the heated zone, we can consider the dynamics governing energy conservation in the gas phase to be quasi-steady state, since the gas and solid temperatures equilibrate rapidly:

$$\varepsilon(\rho C_{pg})v\,\frac{\partial T_g}{\partial x} = hS_a(T_s - T_g) \tag{14}$$

where ε is the void fraction, and S_a is the surface area per unit volume for the electric heater. The energy balance for the solid phase in the heated zone is

$$(1-\varepsilon)(\rho_s C_{ps})\,\frac{\partial T_s}{\partial t} = k_s(1-\varepsilon)\,\frac{\partial^2 T_s}{\partial x^2} + hS_a(T_g - T_s) + \frac{P}{V_H} \tag{15}$$

where the supplementary heat source term P/V_H is the electric power input per unit volume of monolith and k_s is the thermal conductivity of the solid phase.

Since the heated zone and unheated zone are generally separated by a small gas gap, the temperature in the solid phase is not constrained to be continuous. We assume there is no conduction heat transfer between the heated and unheated zones: $\partial T_s/\partial x = 0$ on both sides of the interface. All the gas-phase species concentrations and the gas-phase temperature are continuous at the interface between the two zones.

Table 3 lists the parameters of the electric heater for the system (Keith et al., 2001). By using an electric heater with a power supply of 4.2 kW (a substantial power supply), the maximum gas temperature exiting the heater reaches 679 K. If power supplies are less than 4.2 kW, the filter will fail to ignite.

To solve this problem, an electric heater with greater power dissipation must be used. However, it is not realistic to use this size electric heater, since it draws too much electric power from the battery. One can use another battery, but it will increase the weight of the vehicle and complicate the electrical system. In this article, we work on redesigning the filtration system to solve this problem. With our new bypass filtration system design, we can use a low-power electric heater to raise the exhaust gas temperature above 679 K and hence guarantee filter ignition.

Bypass System

System Configuration

The failure to raise the exhaust gas temperature in the standard system is due to the high flow rate of exhaust gas that occurs under typical driving conditions. From Eqs. 14–15, we know that decreasing the flow rate of exhaust gas will increase the temperature of the exhaust gas exiting the heater. Therefore, the flow rate of the exhaust gas that flows through the electric heater and the filter should be restricted.

Instead of one channel in the standard system, the bypass system will use multiple channels to reduce the flow rate of the exhaust gas that passes through an electric heater, thereby increasing the exhaust-gas temperature above 679 K, thus ensuring ignition in the particulate trap. This system consists of multiple channels in parallel. Each channel is equipped with a particulate filter and an upstream electric heater, placed as close to the filter as possible to avoid heat loss.

System Operation

Basically, the exhaust gas passes through all the channels during both the particle collection and filter regeneration processes. During the regeneration process, the oxygen necessary for combustion is provided by the exhaust flow. With a control

Table 3. Electric Heater Parameters

Parameter	Value
L	0.0254 m
ε	0.8800
$(\rho_s C_{ps})$	2.310×10^6 J/K · m^3
k_s	1.627 J/K · s · m
h	133 J/K · s · m^2
S_a	2283 m^2/m^3
V_H	1.183×10^{-4} m^3

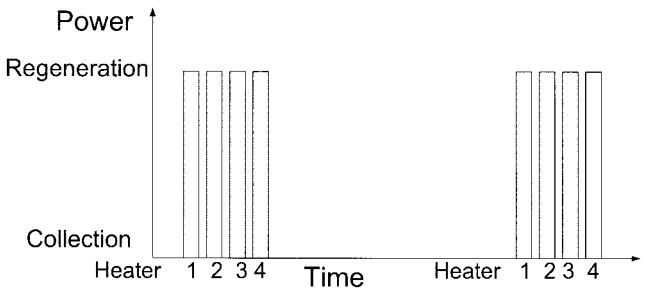

Figure 4. Power cycle of the bypass trap system.

unit, the heaters work independently and the regeneration process is carried out sequentially in each channel. The operation of the bypass system is shown in Figure 4.

Initially, all heaters are off and the particulates are trapped in all channels. When the amount of particulates trapped in the first channel reaches a predetermined level, power is supplied to the heater to warm the exhaust gas in order to initiate combustion in the first filter. The electric heater is kept on until the regeneration process is complete. During this process, the other heaters are off. Immediately after regeneration in the first filter, the second heater is turned on and the second filter is regenerated. This process is repeated until all of the filters have been regenerated. Particulates are then collected as normal until regeneration is needed again.

Simulation Results for New Design

The multiple-channel system described earlier will be implemented in two different designs. The first design reduces the cross-sectional area of both the heater and filter to keep the gas velocity the same as in the standard system. The second design uses the same size heater and filter as the standard system, which significantly decreases the gas velocity.

Constant Gas Velocity. In this design, the cross-sectional area of the heater and filter are decreased in proportion to the number of channels, n. It is noted that the mass flow rate and the initial deposit mass in each channel is smaller by a factor of n. With these exceptions, the standard initial conditions in Table 2 are used in this case. The critical temperature necessary to initiate regeneration is identical in both the standard system and the bypass system, and is equal to 679 K. This is due to an identical cooling effect (heat removal by the exhaust gas).

Figure 5 shows the relationship between ignition time and electric heater power, where the ignition time for regeneration increases with decreasing electrical heater power. At some point, the ignition time goes to infinity, which means there is no ignition during the regeneration process. Therefore, there exists a minimum power requirement for a complete regeneration. As shown in Figure 5, a 2.1-, 1.4-, and 1.1-kW heater is needed to regenerate the filter with two, three, and four channels, respectively. This is because the mass flow rate of gas in each channel decreases due to this bypass design, and thus offers lower power requirements than the standard system.

Figure 6 shows the total energy consumption for a regeneration process in exhaust systems with varying numbers of channels calculated for regeneration in all channels. Compared with the standard system, the increase in the number of channels decreases the mass flow rate in one channel but increases

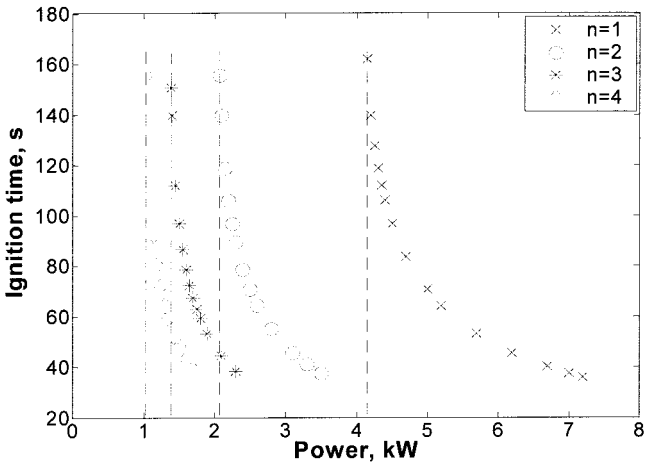

Figure 5. Ignition time as a function of power for the bypass trap system with constant gas velocity.

the total regeneration time. Therefore, the total energy consumption is the same for the standard system with one heater and the bypass system with multiple heaters. This result indicates that the bypass system with a constant gas velocity design does not improve regeneration performance, but just reduces the minimum power requirement.

Constant Heater and Filter Size. In this design, the same size heater and filter are used in the bypass system as in the standard design. This results in a decrease in both the exhaust-gas velocity and mass flow rate in each channel, although it would increase the capital cost. With these exceptions, the standard initial conditions are used in this case. The addition of a second, third, and fourth channel with a heater and filter significantly reduces the critical temperature to 660, 648, and 641 K, respectively. This is because the cooling effect by the exhaust gas on the filter during the regeneration process becomes smaller due to a significant decrease in the exhaust gas velocity.

With the drop in the critical temperature, this design can provide an even lower power requirement than the previous multiple-channel design of the previous subsection. As shown

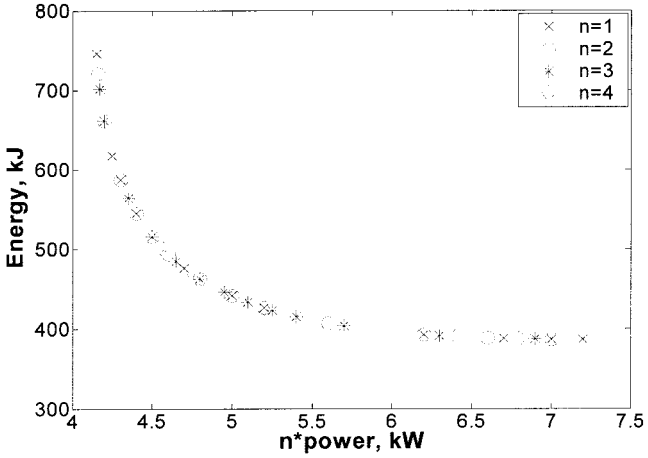

Figure 6. Energy as a function of power for the bypass trap system with constant gas velocity.

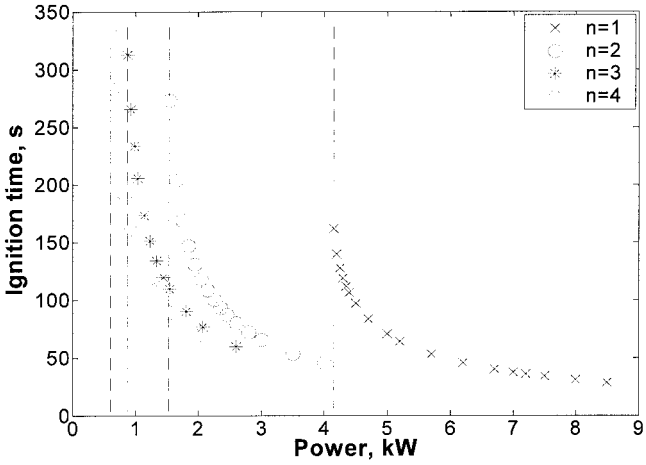

Figure 7. Ignition time as a function of power for the bypass trap system with constant cross-sectional area.

in Figure 7, 1.6-, 0.8-, and 0.6-kW heaters are needed with a two-, three-, and four-channel system, respectively.

Figure 8 shows the total energy consumption for a regeneration process for this design. The constant filter and heater-size design consumes less energy than the standard system. This is a marked improvement over the constant velocity case detailed earlier. The reason is that the decrease in the exhaust gas flow rate reduces the cooling effect and a lower critical inlet temperature is achieved. Therefore, the bypass system with a constant filter and heater-size design provides improved regeneration performance compared to the standard thermal regeneration system.

Analytical Model

Inspection of Figures 2 and 3 shows that there is a large increase in temperature during regeneration. This process can be approximated by two distinct parts: a kinetic limitation (first and second stages, from $t = 0$ to t_{ig}) and a mass-transfer limitation (third stage, from $t = t_{ig}$ to t_{reg}). The kinetic limiting regime is distinguished by a nearly constant deposit

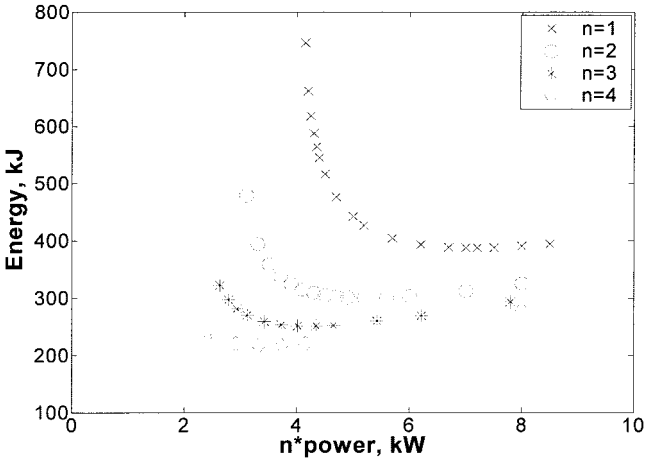

Figure 8. Energy as a function of power for a bypass trap system with constant cross-sectional area.

Table 4. The Values of A and β at Different T_i for the Standard Initial Conditions

T_i (K)	A	β
679	0.02636	23.6555
685	0.03324	23.2430
690	0.04035	22.9014
700	0.05831	22.2596
710	0.08375	21.6370
720	0.1191	21.0403
730	0.1677	20.4878
740	0.2340	19.9184
750	0.3237	19.3908

thickness and oxygen concentration, due to the low reaction rate ($\bar{k} < 1$). The mass-transfer limiting regime is distinguished by a constant slope of the mass vs. time and temperature vs. time graph, due to a high a reaction rate ($\bar{k} \gg 1$). This behavior allows us to decouple the thermal and deposit dynamics and obtain a separate estimate for the ignition time, t_{ig}, and the deposit depletion time, $t_{reg} - t_{ig}$. The first estimate is for the ignition time t_{ig}. In order to obtain an analytical expression, the reaction kinetics are reduced to a zero-order Frank-Kamenetskii form given by $(\overline{\Delta H}\ \overline{k_1} y_0)/\overline{T_0} = Ae^{\beta(T_0-\bar{T}_i)}$. The values of A and β, depending on the initial conditions, can be calculated from the intercept and slope of a plot of $\ln((\overline{\Delta H}\ \overline{k_1} y_0)/T_0)$ as a function of T_0 at the point $T_0 = \bar{T}_i$. Table 4 shows values of A and β at different inlet temperatures $\bar{T}_i$ for the standard initial conditions. This expression can be inserted into Eq. 11 and integrated from a lower limit of $\bar{x} = -w_0(\bar{t} = 0)$ [the initial deposit thickness $w_0(\bar{t} = 0) = 1$ is used at all times, since consumption is ignored] to an upper limit of $\bar{x} = w_s$ to give

$$\frac{dT_0}{d\bar{t}} = \frac{1}{\overline{C_{p2}} \cdot \overline{w_s} + \overline{C_{p1}}} \cdot (A \cdot e^{\beta(T_0-\bar{T}_i)} - \bar{F} \cdot (T_0 - \bar{T}_i)) \qquad (16)$$

By choosing

$$u = \frac{\bar{F} \cdot \bar{t}}{\overline{C_{p2}} \cdot \overline{w_s} + \overline{C_{p1}}}, \qquad \xi = \frac{\beta A}{\bar{F}}, \qquad r = \beta(T_0 - \bar{T}_i)$$

Eq. 16 becomes

$$\frac{dr}{du} = \xi e^r - r \qquad (17)$$

The following conditions hold on r

$$\text{At } \bar{t} = 0, \qquad u = 0, \qquad \text{and} \qquad r = \beta(1 - \bar{T}_i) = r_i.$$

$$\text{At } \bar{t} = \overline{t_{ig}}, \qquad u = u_{ig}, \qquad \text{and} \qquad T_0 = \infty, \qquad r = \infty$$

Integrating Eq. 17 from $u = 0$ to u_{ig}, one obtains

$$\xi u_{ig} = \int_{r_i}^{\infty} \frac{dr}{e^r - r/\xi} \qquad (18)$$

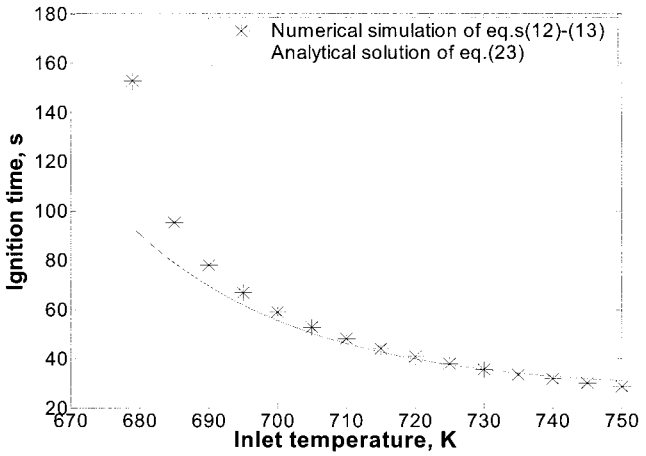

Figure 9. Ignition times simulated and predicted at different feed temperatures.

Since $\bar{T}_i > 1$, r_i is negative. From Table 4, $\beta \gg 1$, such that $|r_i|$ is very large. Thus, we consider an expansion for large $r_i(|r_i| \gg 1)$.

Taking the derivative of Eq. 18 with respect to r_i

$$\frac{d}{dr_i}(\xi u_{ig}) = \frac{d}{dr_i}\int_{r_i}^{\infty} \frac{dr}{e^r - r/\xi} \tag{19}$$

Using the Leibnitz rule, Eq. 19 becomes

$$\frac{d}{dr_i}(\xi u_{ig}) = \frac{\xi}{r_i} \tag{20}$$

Equation 20 can be solved analytically. Integrating Eq. 20 gives

$$\xi u_{ig} = \xi \ln|r_i| + f(\xi) \tag{21}$$

When ξ is small, $f(\xi)$ can be obtained by numerical simulation (Leighton and Chang, 1995), to yield

$$u_{ig} = \frac{2.50}{\xi} + \ln|r_i| - 0.344 \tag{22}$$

Writing Eq. 22 in dimensional terms, and assuming a constant mass flow rate and using $m = \rho_1 S w_b$ for the initial deposit loading yields an expression for the ignition time t_{ig}

$$t_{ig} = \left(\frac{C_{p2}\rho_2 w_s S + mC_{p1}}{C_{pg}F(0)}\right)\left\{\frac{2.50}{\beta A} + \ln\left\{\beta\left(\frac{T_i}{T_b} - 1\right)\right\} - 0.344\right\} \tag{23}$$

With this analytical solution, the ignition time of the regeneration process can be calculated from the system parameters and initial conditions.

As illustrated in Figure 9, the zero-order model compares quite well with the model of Bissett and Shadman (1985) in terms of the ignition time at the standard mass flow rate of 0.0523 kg/s for inlet temperatures in the range of 695 to 750 K. The estimate in Eq. 23 is within 10% for this important range. Below 695 K, the zero-order model estimates faster ignition than that of Bissett and Shadman's model due to the higher heat generation estimated by the zero-order approximation. However, the ignition time for inlet temperatures below 695 K is so long that regeneration consumes too much energy. Temperatures below 695 K are not in the practical interest range. Beyond 750 K, the reaction is so rapid that an accurate estimate of the ignition time is unnecessary. Ideally, the optimal bypass design will preheat the feed to a value within this range. For a lower flow rate (which would occur with the bypass design), the range of temperatures over which this model is accurate would shift (just as the critical temperature shifts as the number of bypass channels increase). Therefore, this analytical estimate can be used with confidence.

The second estimate is for the deposit depletion time $t_{reg} - t_{ig}$. After ignition occurs, the reaction rate is so rapid that convective mass transfer of oxygen controls the process. It is noted from Figure 3 that the slopes of temperature vs. time are all nearly equal during the mass-transfer limiting regime, independent of the feed temperature. One can integrate Eq. 13 with $\bar{k} \gg 1$ to predict the deposit thickness $w_0 = 1 - \bar{M}\bar{F}y_i\bar{t}$ and solve for the time to reach zero thickness

$$\bar{t}_{reg} - \bar{t}_{ig} = \frac{1}{\bar{M}\bar{F}y_i(0)} \tag{24}$$

or in dimensional terms, and assuming a constant mass-flow rate

$$t_{reg} - t_{ig} = \frac{mM_a}{M_c F(0)\, y_i(0)} \tag{25}$$

The regeneration time t_{reg} is obtained by adding Eqs. 23 and 25 together.

Conclusions and Discussion

The simulation results indicate that for the standard mass flow rate of 0.0523 kg/s, a critical inlet temperature of 679 K is necessary to provide regeneration for the standard particulate trap system. The standard system fails to regenerate the filter with less than 4.2 kW of supplied power. The proposed bypass system with constant filter and heater-size design is effective in lowering the critical temperature necessary for regeneration, by as much as 40 K for a four-channel system.

Assuming vehicle operation at the standard initial conditions listed in Table 2, the results of this study can be used to develop an optimum bypass design. Comparisons of Figures 6 and 8 show that using multiple channels with a constant-size heater reduces the total energy requirement. The plots in Figure 8 also indicate a minimum energy at a specific power. For one channel (standard design) the optimum power is 7.2 kW. The total regeneration time is 53.1 s and the energy requirement is 382.3 kJ. Increasing the number of channels reduces the optimum point (two channels: 2.6 kW, 115.4 s, 300.0 kJ; three channels: 1.45 kW, 173.2 s, 251.1 kJ; four channels: 0.83 kW, 260.9 s, 216.5 kJ). Since heater power dissipation should be kept small,

choosing three channels reduces the power by 65% from the 4.2-kW "minimum" described earlier while offering a 34% reduction in energy compared to the optimum with one channel. Choosing two channels still has too large a power requirement, while the addition of a fourth channel yields little benefit.

A zero-order reaction model (Eq. 16) is derived from the Bissett and Shadman (1985) transient model by reducing the reaction kinetics to a zero-order Frank-Kamenetskii form given by $A \cdot e^{\beta(T_0 - T_i)}$. The analytical solution (Eq. 23) predicted by the model is in very good agreement with numerical solutions of the regeneration process, and provides an easy way to predict the ignition time. The model for t_{reg} (Eqs. 23 and 25) predicts optimum power levels for one (6.6 kW), two (2.5 kW), three (1.3 kW), and four (0.8 kW) channels, which is very close to that obtained by numerical simulation.

Acknowledgment

The authors thank the College of Engineering and Graduate School at MTU for financial support.

Notation

A = zeroth-order reaction parameter
C_{pg} = heat capacity of gas, 1.09×10^3 J/kg · K
C_{p1} = heat capacity of deposit layer, 1.51×10^3 J/kg · K
C_{p2} = heat capacity of porous ceramic, 1.11×10^3 J/kg · K
$\bar{C}_{pj}$ = dimensionless heat capacity, $C_{pj}\rho_j/(C_{pg}\rho_1)$
C_{ps} = heat capacity of substrate in electric heater
E/R = activation energy/gas constant, 1.8×10^4 K
$\bar{F}$ = dimensionless mass flow rate of gas, $F(t)/F(0)$
$F(t)$ = mass flow rate of inlet gas, kg/s
$F(0)$ = initial mass flow rate of inlet gas, kg/s
h = heat-transfer coefficient
ΔH = heat of reaction, 3.93×10^8 J/kg mol
$\Delta\bar{H}$ = dimensionless heat of reaction, $-\Delta H/(C_{pg}T_bM_a)$
k_j = rate coefficient for the reaction in region j, m/s
k = rate constant defined by Eq. 3, 596 m/s · K
$\bar{k}_j$ = dimensionless rate coefficient, $(s_1 w_b S p M_a k_j)/[RT_bF(0)]$
k_s = thermal conductivity of heater
L = length of electric heater
M_a = molecular weight of gaseous mixture, 29.0 kg/kg mol
M_c = atomic weight of deposit, 12.0 kg/kg mol
$\bar{M}$ = molecular weight ratio, M_c/M_a
m = initial mass of deposit, g
p = pressure, 101 kPa
P = electric power, W
r = dimensionless temperature, $\beta(T_0 - \bar{T}_i)$
R = gas constant, 8.31 m^3 · kPa/kg mol · K
S = filtration area, 1.63 m^2
S_a = electric-heater surface area, m^2
s_1 = specific area of deposit layer, 5.5×10^7 m^{-1}
T = temperature in the filter, K
$\bar{T}$ = dimensionless temperature, T/T_b
T_b = initial temperature, K
$T_i(t)$ = inlet temperature, K
$\bar{T}_i$ = dimensionless inlet temperature, T_i/T_b
T_0 = the first term of perturbation expansions of $\bar{T}$
T_g = the gas temperature in electric heater, K
T_s = the solid temperature in electric heater, K
t = time, s
$\bar{t}$ = dimensionless time, $F(0)t/m$
u = dimensionless time, $\bar{F}\bar{t}/(\overline{C_{p2}} \cdot \bar{w}_s + \overline{C_{p1}})$
u_{ig} = dimensionless ignition time
v = superficial velocity of gas, m/s
V_H = volume of electric heater, m^3
w = thickness of the particulate deposit layer, m
w_b = initial thickness of the particulate deposit layer, m
$\bar{w}$ = dimensionless wall thickness, w/w_b
w_s = thickness of wall of monolith channel, 4.32×10^{-4} m
$\bar{w}_s$ = dimensionless wall thickness, w_s/w_b
w_0 = the first term of perturbation expansions of $\bar{w}$
x = distance, m
$\bar{x}$ = dimensionless distance, x/w_b
y = mole fraction of oxygen
$y_i(t)$ = mole fraction of oxygen at the inlet
$y_i(0)$ = initial mole fraction of oxygen at the inlet

Greek Letters

β = inverse Frank-Kamenetskii temperature
δ = perturbation variable, $C_{pg}F(0)w_b/S\lambda_1$
ε = void fraction
λ_1 = bulk thermal conductivity of deposit layer, 0.84 W/m · K
λ_2 = bulk thermal conductivity of porous ceramic, 1.1 W/m · K
ρ = density of gas, kg/m^3
ρ_1 = bulk density of deposit layer, 5.5×10^2 kg/m^3
ρ_2 = bulk density of porous ceramic, 1.4×10^3 kg/m^3
ρ_s = density of substrate in electric heater

Subscripts

i = inlet condition
j = 1, 2 = indicating particulate region (j = 1) and ceramic region (j = 2)

Literature Cited

Arai, M., and S. Miyashita, "Particulate Regeneration Improvements on Actual Vehicle Under Various Conditions," *SAE Special Publications,* **816**(2), 10 (1990).

Bissett, E. J., and F. Shadman, "Thermal Regeneration of Diesel Particulate Monolithic Filters," *AIChE J.,* **31**(5), 753 (1985).

Field, M. A., D. W. Gill, B. B. Morgan, and P. G. W. Hawksley, *Combustion of Pulverized Coal,* BCURA Leatherhead, Cheroy and Sons, Banbury, UK (1967).

Howitt, J., and M. Montierth, "Cellular Ceramic Diesel Particulate Filter," SAE Paper 810114 (1981).

Huynh, C. T., J. H. Johnson, S. L. Yang, S. T. Bagley, and J. R. Warner, "A One-Dimensional Computational Model for Studying the Filtration and Regeneration Characteristics of a Catalyzed Wall-Flow Diesel Particulate Filter," SAE Paper 2003-01-0841 (2003).

Igarashi, T., M. Shimoda, T. Otani, K. Tsuchihashi, and M. Shigemori, "Development of Diesel Particulate Trap Systems for City Buses," SAE Paper 910138 (1991).

Keith, J. M., H.-C. Chang, and D. T. Leighton, "Designing a Fast-Igniting Catalytic Converter System," *AIChE J.,* **47**(3), 650 (2001).

Koltsakis, G. C., and A. M. Stamatelos, "Modeling Thermal Regeneration of Wall-Flow Diesel Particulate Traps," *AIChE J.,* **42**(6), 1662 (1996).

Lahaye, J., S. Boehm, Ph. Chambrion, and P. Ehrburger, "Influence of Cerium Oxide on the Formation and Oxidation of Soot," *Combust. Flame,* **104,** 199 (1996).

Leighton, D. T., and H.-C. Chang, "A Theory for Fast-Igniting Catalytic Converters," *AIChE J.,* **41**(8), 1898 (1995).

Muscat, J. E., and E. L Wynder, "Diesel Engine Exhaust and Lung Cancer: An Unproven Association," *Environ. Health Perspect.,* **103,** 812 (1995).

Manuscript received Dec. 13, 2002, and revision received May 27, 2003.